

# Measurement of instantaneous 2-D velocity field and local chemiluminescence in a premixed-spray flame by PIV and MICRO system

by

Shohji TSUSHIMA\*, Masaaki NEGORO\*, Hiroyasu SAITOH\*  
Manabu FUCHIHATA\*\*, Fumiteru AKAMATSU\* and Masashi KATSUKI\*

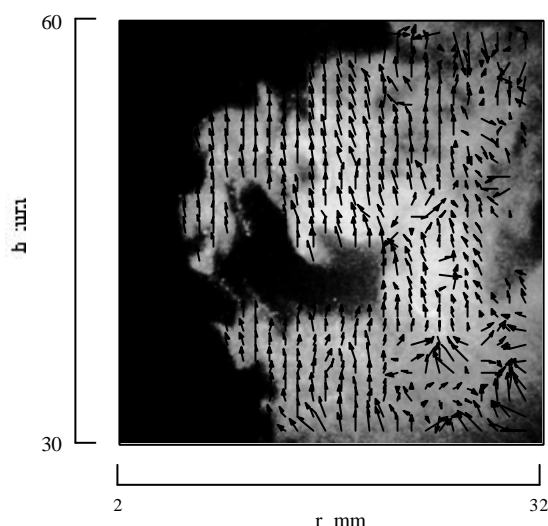
\*Department of Mechanical Engineering, Osaka University  
2-1 Yamada-oka, Suita, Osaka 565-0871 JAPAN

\*\*Department of Mechanical Engineering, Kinki University  
3-4-1 Kowakae, Higashi-Osaka, Osaka 577-8502, JAPAN

## ABSTRACT

In this article, combined measurements of particle image velocimetry (PIV) and Multi-colour Integrated Cassegrain Receiving Optics (MICRO) are demonstrated in an attempt to investigate characteristics of propagating flame in a premixed-spray stream. The cross-correlation PIV system consisting of an Argon-ion laser and a CCD camera with an image intensifier showed its capability to provide instantaneous two-dimensional (2D) velocity fields in sooty spray flames as shown in Fig.1, where liquid fuel of kerosene was supplied in the form of premixed-spray. It enabled us to give a more detailed interpretation of the influence of fluid turbulent motion on the process of *preferential* flame propagation. Furthermore, local chemiluminescences in flames detected by MICRO system were conditionally processed in terms of the distance from spray boundary that was calculated from the visualized spray images. The obtained one-dimensional flame structure in the direction of flame propagation showed that two

Fig.1 2-D velocity fields with spray



distinct reaction peaks appeared on both side of the main vaporization region.

## 1. INTRODUCTION

Flame propagation in sprays is a unique character of spray combustion (Myers and Lefebvre, 1986; Roth *et al.*, 1996). Intensive efforts have been made to investigate premixed-like behaviour in spray flames by several researchers (Hayashi *et al.*, 1976; Richards and Lefebvre, 1989; Greenberg *et al.*, 1996). Since spray flames are heterogeneous turbulent reacting two-phase flows, they have inherently complicated transient structures. Adding that, inhomogeneity of spray properties in space and time gives further complexity to spray flame characteristics. To clarify the characteristics, the instrumentation of high resolution in both space and time is strongly required.

In our recent experiments, we observed time-series behaviour of spray flame in a premixed-spray burner using laser tomography consisting of a high speed CCD camera and an Argon-ion laser, and found that a portion of premixed-spray stream issued from a burner-port rapidly disappeared in radial direction (Tsushima *et al.*, 1998). We thought that such a rapid disappearance of spray stream was caused by the propagation of flame, which preferentially intruded into a easy-to-burn part of premixed-spray stream, although the influence of turbulence associated with large eddies was not fully investigated. Turbulent motion in shear layers between the premixed-spray stream and the air in environment may possibly fluctuate flame surface as seen in gaseous premixed turbulent flames (Chew *et al.*, 1989) and cause the displacement of droplets moving out of the probing laser-sheet.

In the present study, a cross-correlation type PIV system consisting of an Argon-ion laser and a CCD camera coupled with an image intensifier was applied to the same premixed-spray burner in order to obtain two-dimensional (2D) instantaneous velocity fields to clarify the influence of turbulent motion on flame propagation processes. To ensure the ability of the PIV system in spray flames with bright luminosity, the obtained velocity fields were also compared with those measured by phase-Doppler anemometry (PDA).

Point-wise measurement of local chemiluminescence of OH- and CH-radicals together with Mie scattering from illuminated droplets in the flame was also conducted simultaneously using MICRO probe system (Akamatsu *et al.*, 1999) to examine the flame structure in the direction of flame propagation. One-dimensional structure of the propagating flame was obtained by the combined data processing of both images and point-wise signals.

## 2. EXPERIMENTAL APPARATUS

The experimental apparatus used in the study is shown in Fig.2. The detailed configuration of premixed-spray burner and flame photograph can be found elsewhere (Akamatsu *et al.*, 1997). Flow configuration is thus briefly given here. Liquid fuel of kerosene was injected through an twin-fluid atomizer which was placed 440 mm upstream from the burner port to form a premixed-spray stream,

almost uniformly suspended droplets in the air supplied as carrier gas. This unique configuration produces low slip velocity between suspended droplets and air because most of large droplets are eliminated in the mixing chamber. The spray flame was anchored by an annular pilot burner of hydrogen diffusion flame that was formed around the burner port.

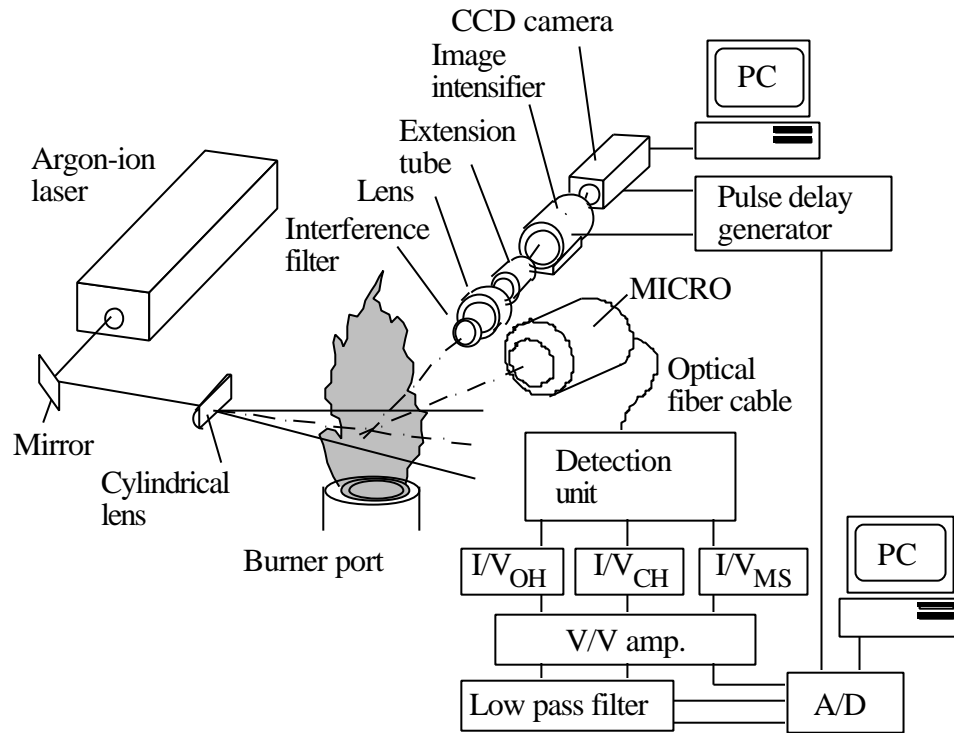


Fig. 2 experimental apparatus

To illuminate fuel droplets, an Argon-ion laser (Spectra Physics, Stable 2017, Maximum output power 4W) was used in the present study, instead of a costly double-pulsed laser that are often used to freeze fluid motion of interest in PIV measurement. A thin laser light sheet, 0.5 mm thickness, was formed by a cylindrical lens and illuminated vertical plane above the burner port. Since we adopted the continuous wave Argon-ion laser as a light source, an image intensifier (Hamamatsu, C6653) was utilized as an electrical shutter to control exposure time. Adding the fact above, the image intensifier was also essential in this experiment to suppress background luminosity from sooty flames.

A CCD camera (Kodak, Megaplus Model ES 1.0) coupled with the image intensifier was used to record spray images. The “triggered dual exposure mode” originally installed in the camera can take two consecutive images with minimum separation time of 5  $\mu$ s. The mode seems also useful when it is coupled with a pulsed-laser as demonstrated by Lourenco *et al.*, 1996, and Thurber *et al.*, 1998.

The TTL pulse timing diagram for the PIV measurement is shown in Fig. 3 together with the exposure time chart of the CCD camera. The exposure time for the first image on the CCD camera is controllable up to 255  $\mu\text{s}$  at the maximum by a provided software with the CCD camera. In contrast, the exposure time for the second image on the CCD camera is fixed at 33 ms, which seems considerably long in terms of instantaneous imaging of flame in the present experiment. Therefore, the coupled image intensifier on the CCD camera worked primarily as an electrical shutter to control actual exposure time for the CCD camera.

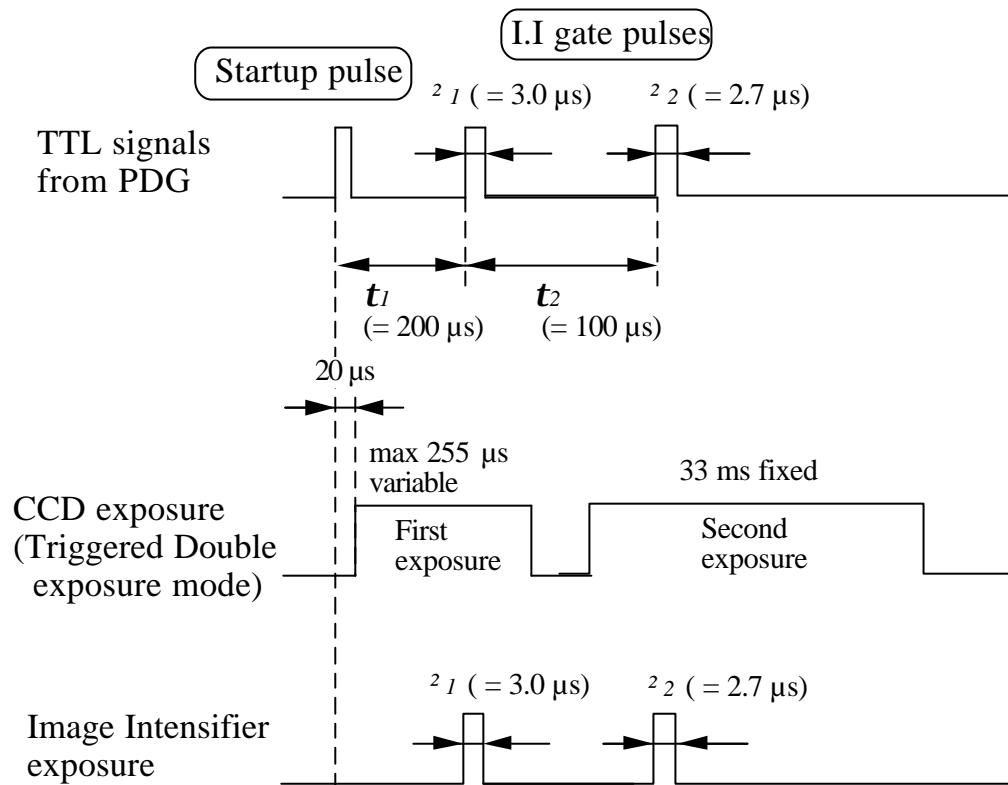


Fig. 3 Pulse and exposure time chart for PIV measurement

The pulse sequence employed for the PIV imaging in the present study is as follows. Totally three TTL signals generated by a pulse delay generator (PDG) (Stanford Research Systems, WC Model DG535) were used to obtain two consecutive images. The first TTL signal named “*startup pulse*” is supplied to the CCD camera to trigger an acquisition of pair of images. Image acquisition for the first frame is to start at least  $20 \mu\text{s}$  after the *startup pulse*. Then, the second and the third pulse of TTL signals are supplied to the image intensifier to open the electrical shutter with specified time duration,  $t_1$  and  $t_2$ . The exposure time for the electrical shutter can be controlled by input pulse widths,  $t_1$  and  $t_2$ .

In the present study, the width and time duration of input TTL signals were carefully chosen in order to take two consecutive spray images with equal image brightness. The adopted pulse sequence is shown

in the Fig. 3 in which the width of third pulse is 2.7  $\mu\text{s}$ , which is slightly shorter than that for the second pulse of 3.0  $\mu\text{s}$ . The delicate difference was determined by try-and-error optimization, since the pixel intensity of the second image was slightly higher than that of the first image if we used the same exposure time of 3.0  $\mu\text{s}$ .

The imaged area was a square of 30 mm by 30 mm, which corresponds to  $h= 30$  mm to 60 mm and  $r = 2$  mm to 32 mm, where  $h$  and  $r$  denote axial and radial distance measured from the center of the burner port, respectively. Mie scattering signals from illuminated droplets were collected onto 1008 pixels by 1018 pixels on the CCD array through a 514.5 nm  $\pm$  1.8 nm optical interference filter to suppress spontaneous emissions from the flame. It should be noted that the displacement of droplets due to convection of the flow during the exposure time is negligible. The estimated displacement of droplets during two consecutive images from the measured axial mean velocity of droplets by a phase Doppler velocimeter is approximately 20 pixels which corresponds to 0.6 mm in actual space.

To derive instantaneous velocity fields of the premixed-spray, the obtained images were firstly reduced into 1/3-size frame to lessen calculation load on the computer. Consequently, the resultant spatial resolution of 1/3 image was 336 pixels  $\times$  340 pixels. Then, cross-correlation method was applied to the reduced images. The size of reference circle for the calculation of cross correlation in the image processing was chosen 1.5 mm, which was equal to about 17 pixels.

Adding to the PIV measurement, monitoring of local chemiluminescence underlying in OH- and CH-bands, the monitored wavelength of which were 308.5 nm and 430.5 nm respectively, and Mie scattering was simultaneously measured using Multi-colour Integrated Cassegrain Receiving Optics (MICRO) system. The details of the configuration with experimental and numerical validation of the system have been reported by Akamatsu *et al.*, 1999. The brief description on this monitoring system is thus given here.

Each emission is collected by the MICRO probe and is guided into a detection unit through an optical fiber. Three set of interference filter and photomultiplier (PMT) (Hamamatsu, R106UH) are allocated to respective wavelength in the detection unit, and electric current signals from each PMT are amplified after conversion into voltage and digitized by an A/D converter (Elmec, EC-2390) with sampling rate of 100 kHz.

In preliminary experiments, we confirmed that the MICRO system had the potential to detect local chemiluminescence with spatial resolution smaller than 4 mm long and 2 mm in diameter.

### 3. RESULTS AND DISCUSSION

#### **3.1 Influence of turbulence on preferential flame propagation.**

Figure 4 presents a sample image of visualized premixed-spray flame where an instantaneous velocity field obtained by PIV is superimposed. As seen in the figure, a portion of spray region is eroded into a concave-shaped boundary, which will be referred as *concavity* in the following. In our previous study, the formation process of such a *concavity* was observed on time-series tomographic spray images recorded by a high-speed CCD camera (Tsushima *et al.*, 1998). However, it was not clear whether the rapid disappearance of a portion of premixed-spray stream was caused by the flame propagation or by turbulent motions of the flow. In Fig. 4, the instantaneous velocity field obtained by the PIV measurement demonstrates that most of velocity vectors inside the spray region (white zone) have the same orientation as  $h$  axis.

As the result of careful observation on velocity vectors in the vicinity of periphery of the spray region, turbulent motions associated with large eddies were not identified. Accordingly, turbulent motion does not seem to be an influencing factor on the rapid disappearance of a portion of the premixed-spray stream. It is confirmed that rapid disappearance of a premixed-spray stream is caused by rapid vapourization of fuel droplets, which is accompanied with flame propagation. The propagating flame formed in the premixed-spray preferentially intrudes into an easy-to-burn region so that we call this behaviour *preferential* flame propagation.

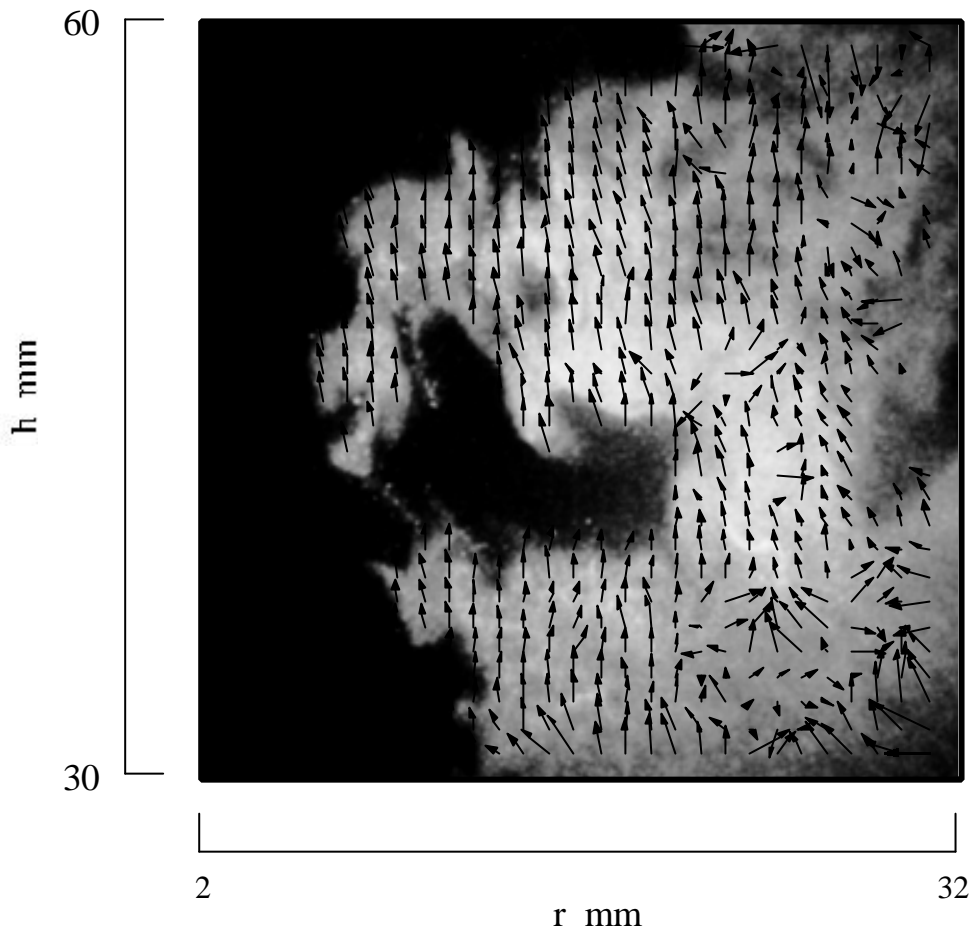


*Fig. 4 Instantaneous velocity field measured by the PIV system.  
Visualized spray is superimposed.*

### **3.2 Comparison with PDA results**

To examine the performance of the present PIV system, velocity vectors obtained by PIV were compared with those measured by a phase-Doppler anemometry (PDA). Figure 4 shows mean velocity vectors, which were measured by PIV (Fig. 5 (a)) and PDA (Fig. 5(b)), respectively. The one-dimensional PDA system (Dantec, transmitter 60X; receiver 57X10 and signal processor 58N10) was employed in this experiment. The number of sampled droplets at each measuring point in PDA measurement was 3000 so that a few seconds was enough for the data acquisition at each point. On the other hand, the presented results by PIV experiment was obtained by averaging a set of 300 velocity fields.

As shown in Fig. 5, velocity vectors measured by PIV are in excellent agreement with those by PDA measurement. It is confirmed that the PIV system used in this study shows its high ability to measure velocity fields in the premixed-spray flame.

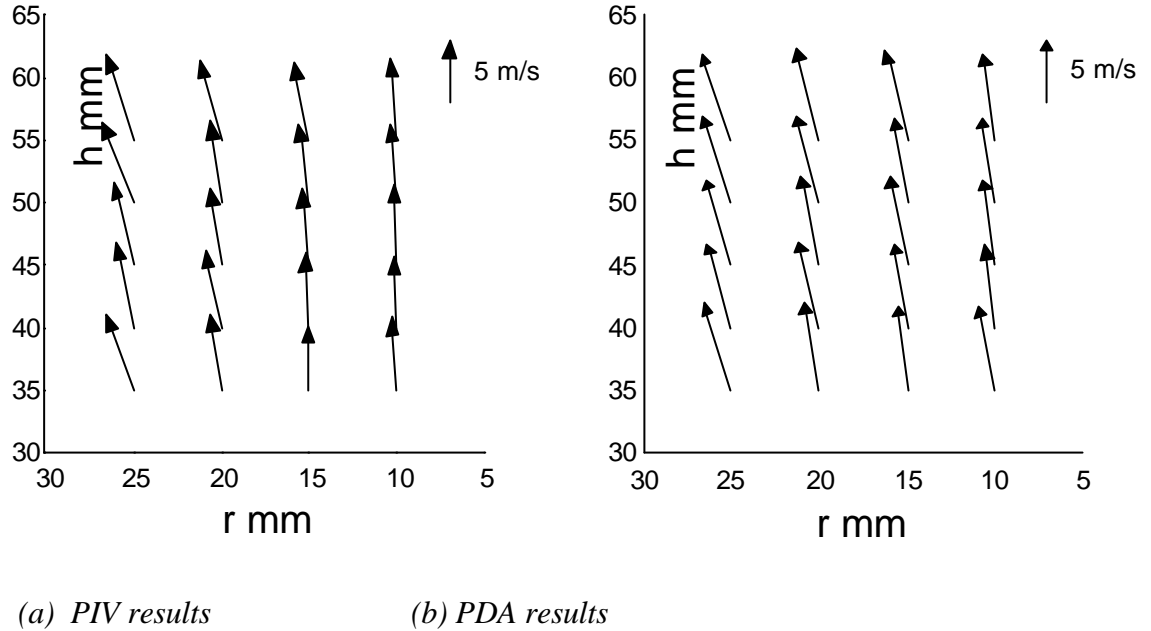


Fig. 5 Comparison of mean velocity vectors measured by PIV and PDA experiments

### 3.3 One-dimensional structure of propagating flames in spray

One dimensional structure of a propagating flame in the direction of propagation was examined by the combination of image and signal processing. The data deduction procedure was as follows. Using MICRO optics, we collected light emissions originating from the measuring point on the plane of laser-sheet, which is the focal point of the MICRO shown by a closed circle in Fig.6. Measured signal intensities of OH- and CH-band and Mie scattering in the case of Fig. 5 were 7.93 nA, 308.3 nA and 20.85  $\mu$ A, respectively. Then, the spray image was binarized to define spray boundaries. The resultant spray boundaries are shown in Fig. 6. As a result, *reference distance* from the focal point of MICRO probe to spray boundaries,  $L$ , can be estimated 1.11 mm as illustrated in Fig. 6.

The intensity distribution of each signal in terms of the *reference distance* was obtained by averaging totally 300 runs in an attempt to deduce mean one-dimensional structure of propagating flame. Figure 7 shows mean signal intensities of Mie scattering and OH- and CH-band emissions along the *reference distance*. The negative value of *reference distance* means the measurement point of MICRO probe located outside the spray boundary where the number density of fuel droplet abruptly decreases due to vapourization. Judging from the figure, the intensity of Mie scattering shows its maximum gradient at  $L = 0$  mm, and completely attenuates at  $L = -2$  mm. This fact indicates that the evaporation of fuel droplets is intense at spray boundary defined by the binarization of the spray images. Accordingly, the

spray boundary defined by the image processing represents the main vaporization plane in spray flames.

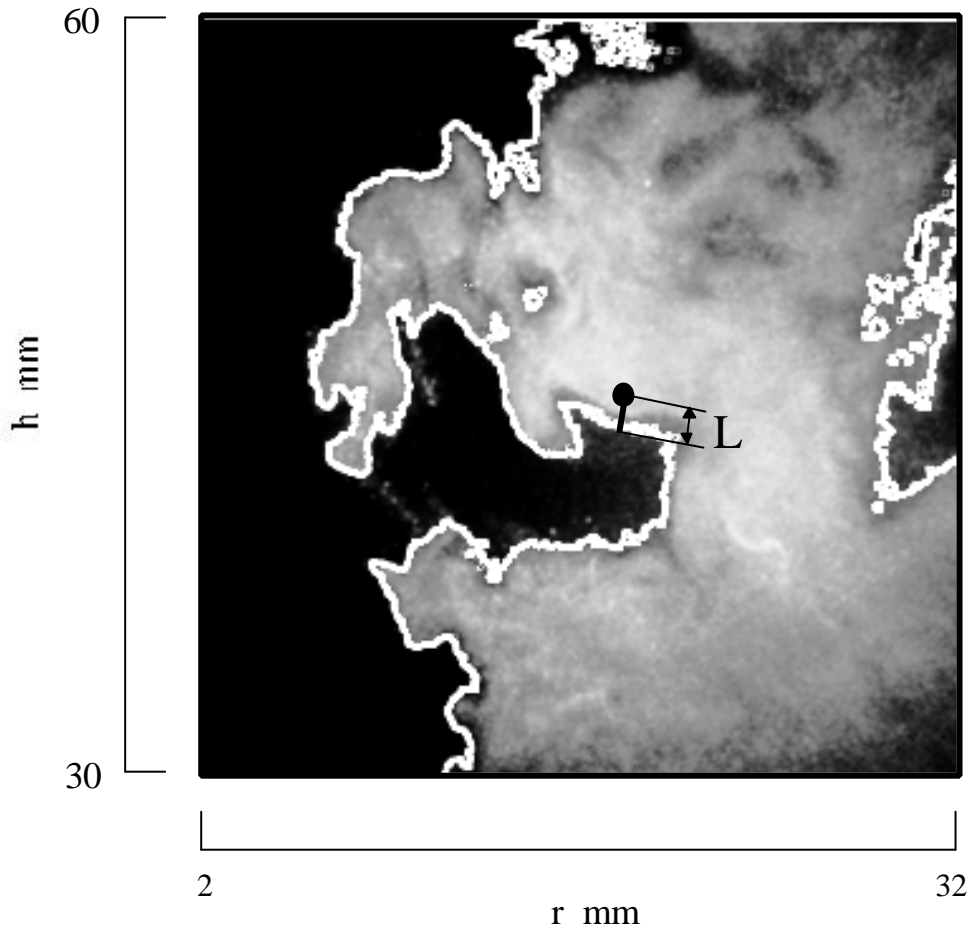
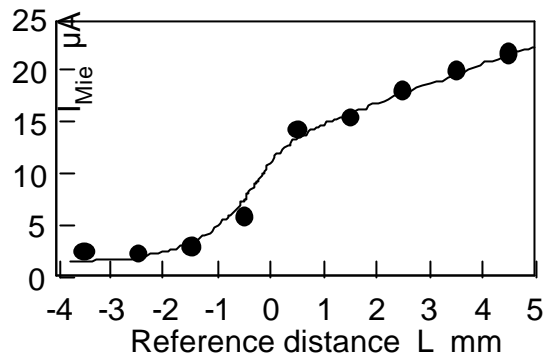
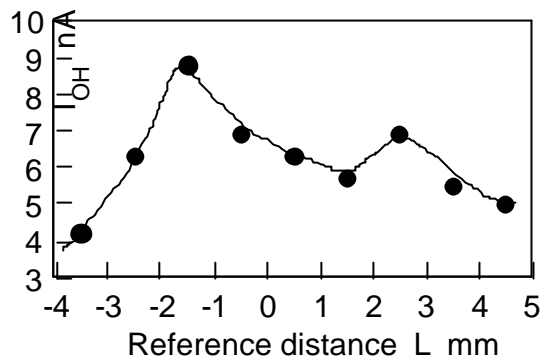


*Fig. 6 The contours of the spray boundary obtained by binarizing the spray image. A closed circle indicates the measurement location of MICRO probe system.*

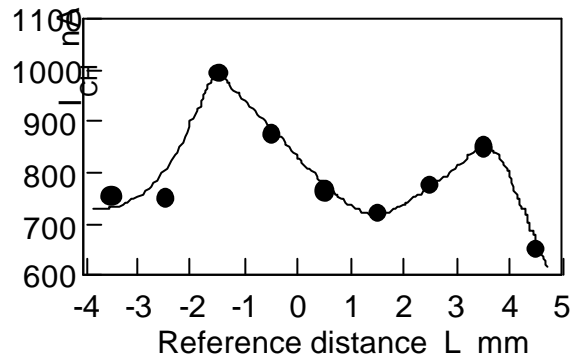
In Fig. 7 (b) and (c), two distinct peaks of OH- and CH-band emissions can be identified. Physical interpretation on these chemiluminescence, which are considered to be good markers to identify the existence of reaction zone, are given in the literature (Gaydon, 1974). It shows that intensive reaction regions exist on both side of main vaporization plane. This sort of two-stage flame structure in spray flames was reported by Li and Williams, 1996, and Continillo and Sirignano, 1990. However, further investigation will be necessary to clarify instantaneous structure of the propagating flame, since the demonstrated results in the present study are time-averaged.



(a) Mie scattering emissions



(b) OH-band emissions



(c) CH-band emissions

*Fig. 7 Profiles of averaged signal intensity along the reference distance.  
Plotted in the figure are the results obtained from the total 300 tests*

#### **4. CONCLUSIONS**

In order to clarify influence of turbulent motion on rapid disappearance of the premixed-spray stream, particle image velocimetry (PIV) consisting of an Argon-ion laser and a digital CCD camera coupling with an image intensifier were applied to the premixed-spray burner. As a result, no turbulent motion associated with large eddies were identified when a portion of premixed-spray stream was abruptly intruded. It was thus confirmed that flame preferentially propagated into an easy-to-burn region of the premixed-spray stream, which was named *preferential flame propagation*.

Furthermore, in order to deduce one-dimensional structure of the propagating flame along the direction of propagation, OH- and CH-band emissions and Mie scattering were measured by MICRO probe system together with spray images. It was shown that combination of both signal and image processing, which was demonstrated in the present study, can provide one-dimensional mean structure of the flame. It was also suggested that two distinct reaction region existed on both sides of the main vaporization region.

#### **ACKNOWLEDGEMENTS**

This research was partially supported by the Grant-in-Aid for Scientific Research, the Ministry of Education, Science and Culture, Japan. The authors would like to acknowledgement the financial support of Japan Society for the Promotion of Science through Research Fellowships for Young Scientists.

#### **REFERENCE**

Akamatsu, F., Mizutani, Y., Katsuki, M., Tsushima, S. Choi, Y. D. and Nakabe, K., Atom. Sprays, 7-2:199-218(1997).

Akamatsu, F., Wakabayashi, T., Tsushima, S., Katsuki, M., Mizutani, Y., Ikeda, Y., Kawahara, N. and Nakajima, T., Meas. Sci. Tech., 10:1240-1246(1999).

Chew, T. C. Britter, R. E. and Bray, K. N. C., Combust. Flame, 75:165(1989).

Continillo, G. and Sirignano, W. A., Combust. Flame, 81:325(1990)

Gaydon, A. G., The Spectroscopy of Flames, Chapman and Hall, London, 1974.

Greenberg, J. B. , Silverman, I. and Tambour, Y., Combust. Flame, 104:358-368(1996).

Hayashi, S., Kumagai, S. and Sakai, T., Combust. Sci. Tech, 15:169-177(1976).

Kodak, User's Manual Model ES 1.0, 1996.

Li, S. C. and Williams, F. A., 26th Symp. (Int.) on Combust., The Combust. Inst., Pittsburgh, PA, 1996, p.1017.

Myers, G. D. and Lefebvre, A. H., Combust. Flame, 66:193-210(1986).

Richards, G. A. and Lefebvre, A. H., Combust. Flame, 78:299-397(1989).

Roth, N., Karl, A., Anders, K. and Frohn, A., 26th Symp. (Int.) on Combust., The Combust. Inst., Pittsburgh, PA, 1996, p.1697.

Thurber, M. C., Kirby, B. J. and Hanson, R. K., 36th AIAA Aerospace Sciences Meeting and Exhibit, 1998, AIAA98-0397.

Tsushima, S., Saitoh, H., Akamatsu, F. and Katsuki, M., 27th Symp. (Int.) on Combust., The Combust. Inst., Pittsburgh, PA, 1998, p.1967.